Thermal Behavior and Kinetic Analysis of the Chain Unfolding and Refolding and of the Concomitant Nonpolar Solvation and Desolvation of Two Elastin-like Polymers

Javier Reguera,[†] José M. Lagarón,[‡] Matilde Alonso,[§] Virginia Reboto,[§] Blanca Calvo,[†] and José Carlos Rodríguez-Cabello*[,†]

Dpto. Física de la Materia Condensada, Universidad de Valladolid, Paseo del Cauce s/n, 47011 Valladolid, Spain; Packaging Lab, IATA-CSIC, Apd. Correos 73, Burjassot 46100, (Valencia), Spain; and Dpto. Química Analítica, E.U.P., Universidad de Valladolid, Francisco Mendizabal 1, 47014 Valladolid, Spain

ABSTRACT: Water-induced chain dynamics alterations are of paramount importance in many protein-based polymers because they determine and affect to a great extent the temperature dependence of the end properties. In this study, the thermal behavior of the reversible unfolding and refolding of poly(Val-Pro-Gly-Val-Gly) and poly(Val-Pro-Ala-Val-Gly) and of their concurrent dehydration and hydration processes has been studied by differential scanning calorimetry (DSC) and turbidimetry. Contrary to the good reversibility shown by poly(Val-Pro-Gly-Val-Gly), the substitution of glycine by alanine in poly(Val-Pro-Ala-Val-Gly) perturbed to a large extent the process of chain unfolding. For the latter polymer, it was found that both chain unfolding and rehydration processes take place at large undercoolings, suggesting that both events occur far from equilibrium conditions and, therefore, are strongly dominated by kinetics. In this context, the existence of an hydration excess with a kinetic rather than a thermodynamic nature is a remarkable observation. The kinetics of folding and unfolding were also studied by using an isoconversional method of kinetic analysis, i.e., the model-free Friedmand's isoconversional method. As expected, the kinetics of the solvation of nonpolar moieties for both polymers indicated a complex and multistep process. Again, poly(Val-Pro-Ala-Val-Gly) showed a quite different pattern characterized by an acute hysteresis behavior which seems to govern the hydration process for this polymer. The differences observed between both polymers have been interpreted in terms of the hindrance provided by the methyl group in alanine during temperature-induced chain dynamics.

Introduction

Because of its unique properties, water drives many processes involving synthetic and natural macromolecules. While a detailed understanding of its precise role is still being unraveled, it is clear that the existence of water shells around biomolecules and nonnatural compounds plays a crucial role. Much effort has been devoted to the study of the structure and dynamics of water of hydration of biomolecules and other compounds. Nevertheless, an extensive part of the work done comes from theoretical calculations such as molecular dynamics simulations on aqueous solutions of proteins (see, for example, refs 1−4), the experimental work being scarce. Among the experimental evidence on the structure and characteristics of the hydration phenomena, dielectric relaxation has proven to be a powerful tool (see, for example, ref 5). Some other techniques such as X-ray diffraction[6] and others have also been applied to this topic. Among the different types of hydration, two extremes can be considered, i.e., the hydrophilic hydration and the nonpolar solvation (NPS), currently named also "hydrophobic hydration". We report in this study about the latter type.

NPS has been considered to play a relevant role in polymer functioning, folding, and self-assembly for decades, particularly in proteins.[7−11] Nevertheless, the experimental approach to this type of hydration has been complex, and not many contributing studies can be found in the literature. There are a number of reasons for this lack of relevant experimental work.[12] A first reason is that only a small part of the hydration is caused by the presence of hydrophobic groups on the surface of the native proteins and other nonnatural polymers. Moreover, the transitions to hydrophobically unfolded states ("cold denaturation") would have to occur under conditions where a substantial part of the total water is involved in the NPS process. Finally, the transitions would have to be thermally accessible and well characterized as being dominantly hydrophobic. Fortunately, characterization of waters of NPS has become accessible by the use of a new class of synthetic polypeptides, the elastin-like polymers.[12] These polymers are made by repeating certain tetra-, pepta-, hexa-, ..., -peptides found in the natural elastin.[13] Poly(Val-Pro-Gly-Val-Gly) is the most renowned of this group of synthetic polypeptides. This polymer can be considered as a predominantly hydrophobic polypeptide, as it can be deduced by its amino acid composition. By substituting some of the amino acids of the pentamer, different polymers have been produced with expanded characteristics. The most successful family of elastin-like polymers is based on modifications of the base pentamer Val-Pro-Gly-Val-Gly, especially those with general formula poly(Val-Pro-Gly-X-Gly), where X represents any natural or modified amino acid. The substitution of any of the other amino acids in the pentamer is not so

[†] Dpto. Física de la Materia Condensada, Universidad de Valladolid.
[‡] IATA-CSIC.
[§] Dpto. Química Analítica, Universidad de Valladolid.
* To whom correspondence should be addressed: e-mail cabello@eis.uva.es.

straightforward. For example, the first glycine cannot be substituted by any other amino acid different from alanine.[13] This is because, according to Urry,[13] there is a type II β-turn per pentamer that involves this glycine in the folded state of the polymer. The presence of bulky moieties in amino acids with L chirality impedes the formation of the β-turn, and the resulting polymer is not functional. Thus, the substitution by alanine is the only possibility reported that still leads to a functional polymer, though even in this case the resulting polymer shows significantly different and "out of trend" mechanical and thermal properties.

All these functional elastin-like polymers exhibit phase transitional behavior.[13] Thus, below the transition temperature (T_t), the polymer chains remain disordered, relatively extended, in solution if they are not cross-linked, and fully hydrated mainly by NPS. On the contrary, above T_t, elastin-like polymers hydrophobically refold and assemble to form a segregated phase in which, according to Urry,[13] the polymer chains adopt an ordered structure, the β-spiral, formed by the concatenation of repeated type II β-turns in each pentamer and the stabilization of the resulting spiral by interturn hydrophobic contacts. In this folded state, the chain loses all the ordered structures of NPS.[13] In the β-spiral state, there may also be some chances of forming interchain hydrophobic contacts, allowing folded chains to first self-assemble in fibrilar nanoparticles and eventually segregate from the solution.[13] In many cases, these particles further aggregate to form a dense phase called "coacervate".[13] This is the result of the so-called "inverse temperature transition" (ITT). Although, in some aspects, ITT shares many features with the so-called "lower critical solution temperature" (LCST) exhibited by other polymers, its differences make more preferable the use of the term ITT for elastin-like polymers.[14]

NPS of poly(Val-Pro-Gly-Val-Gly) and of some other related polymers was characterized by Urry and other groups using microwave dielectric relaxation (MDR)[12] and calorimetric methods such as DSC.[13,15] DSC has proven to be especially indicated to collect such kinds of information. For example, DSC experiments have highlighted that the NPS structures exhibit heterogeneous populations, i.e., from well ordered to poorly ordered structures, varying across the NPS shell.[15]

Most of the knowledge gathered on the NPS of elastin-like polymers comes from the study of the folding−dehydration process. The lack of direct studies on both the unfolding and the concomitant morphological development of the NPS structures has been recently pointed out in the literature.[16] This work intends to shed some light into this not so well characterized phenomena. In particular, the kinetics of the formation of the NPS shell have been never studied neither for these model polypeptides nor for any other relevant natural or nonnatural compounds. This work aims to fill this lack by applying a model-free isoconversional method of kinetic analysis, i.e., the Friedman's isoconversional method, for the study of the kinetics of both the formation and development of NPS structures and their destruction. Isoconversional and multiheating rate methods have demonstrated to yield reliable information on the kinetics of complex processes in condensed phases.[17,18] These techniques cover the vast majority of kinetic studies of thermally stimulated reactions such as decomposition, oxidation, reduction, or crystallization of solids.

Two elastin-like polymers were chosen for this work, namely, poly(Val-Pro-Gly-Val-Gly) and poly(Val-Pro-Ala-Val-Gly). Poly(Val-Pro-Gly-Val-Gly) have been first included in this study because it is considered as a representative model of the whole family of elastin-like polymers,[13] and the results may then be of general significance for other polymers and natural and non-natural polypeptides. Poly(Val-Pro-Ala-Val-Gly) was also included because this material has some particular interesting characteristics, which make it atypical within the family of elastin-like polymers.

Experimental Section

Materials. Poly(Val-Pro-Gly-Val-Gly) was synthesized in our laboratory following the methods described earlier.[19] Detailed characterization of the final polymer can be found in refs 15 and 20. The poly(Val-Pro-Gly-Val-Gly) used in this work has an apparent mean molecular weight (M_n) of 96 155 and a polydispersitivity (n) of 1.18.

Poly(Val-Pro-Ala-Val-Gly) was synthesized following the method described in ref 19. Stoichiometry and purity were routinely checked by ^{13}C and ^{1}H NMR, elemental and amino acid analysis, and chromatographic methods. Verification of the final product was done by NMR and amino acid analysis. ^{1}H and ^{13}C NMR spectra are given in Figure 1. The assignments of resonances are all indicated, and these, with the presence of all requisite peaks and the absence of extraneous peaks, verify the synthesis and purity of the product. In addition, amino acid analysis of the polymer showed the expected composition within the experimental error (result not shown). The apparent average molecular weight and its distribution have been estimated by size exclusion HPLC, as described for poly(Val-Pro-Gly-Val-Gly) in refs 15 and 20. The result of this analysis is plotted in Figure 2.

Differential Scanning Calorimetry (DSC). DSC experiments were performed on a Mettler Toledo 822e with liquid nitrogen cooler. Calibration of both temperature and enthalpy was made with a standard sample of indium. For DSC analysis, 125 mg mL^{-1} polymer solutions were prepared. In a typical DSC run, 20 μL of the solution was placed inside a standard 40 μL aluminum pan hermetically sealed. The same volume of water was placed in the reference pan. Both types of samples were preheated 5 min at 5 °C before the heating measurements and for 1 min at 60 °C before cooling experiments. The heating and cooling rates used for kinetic analysis were 30, 24, 20, 16, 12, 8, 4, 2, −24, −20, −16, −12, −8, −4, and −2 °C min^{-1}.

Turbidity. Turbidity experiments were conducted in a Varian Cary 50 UV−vis spectrophotometer with a thermostatized sample chamber. Turbidity was assessed by the change in absorbance at 300 nm for a 32.1 mg mL^{-1} polymer solution. At a given temperature, the sample was left until a constant turbidity value was reached. This steady value is considered as the actual turbidity for the sample at that temperature.

Kinetic Analysis. The kinetics of thermally stimulated reactions in the condensed phase can be described by the basic equation[21]

$$\frac{d\alpha}{dt} = k(T)\, f(\alpha) \tag{1}$$

where α is the conversion degree (or extent of reaction), t the time, T the temperature, $f(\alpha)$ the reaction model, and $k(T)$ the Arrhenius rate constant, which is given as

$$k(T) = A \exp\left(\frac{-E_a}{RT}\right) \tag{2}$$

where R is the gas constant and A and E_a are Arrhenius

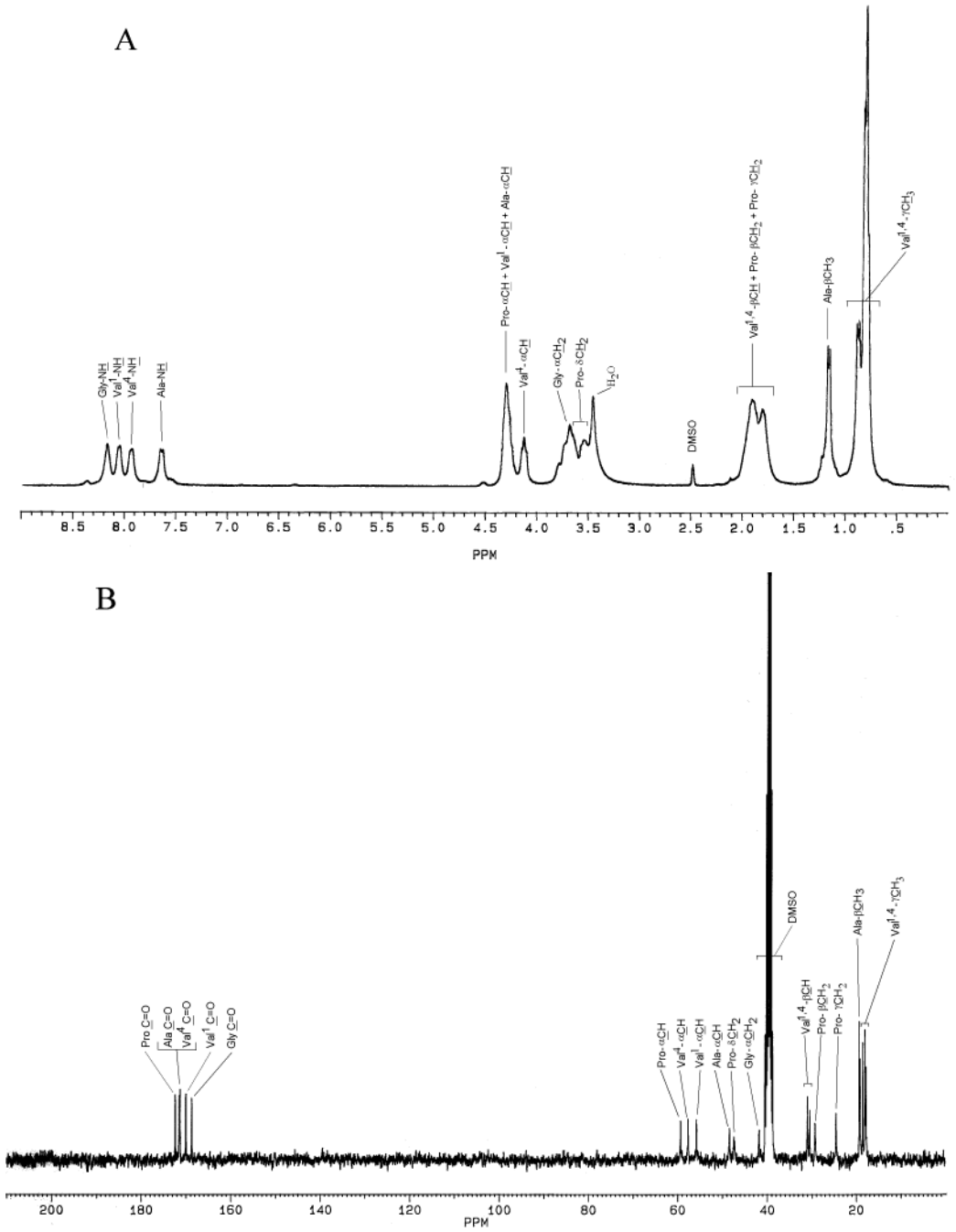

Figure 1. NMR spectrum of poly(Val-Pro-Ala-Val-Gly) in DMSO-d_6: (A) ^{1}H NMR; (B) ^{13}C NMR.

parameters, the preexponential factor and the activation energy, respectively.[22,23]

Reaction kinetics can be studied under isothermal as well as under nonisothermal conditions. For nonisothermal kinetics these processes are usually studied under conditions of a constant heating rate $\beta = \mathrm{d}T/\mathrm{d}t$. For these conditions, combination of eqs 1 and 2 gives[24]

$$\frac{\mathrm{d}\alpha}{\mathrm{d}T} = \frac{A}{\beta} f(\alpha) \exp\left(\frac{-E_a}{RT}\right) \tag{3}$$

which can be written in a logarithmic way:

$$\ln\left(\frac{\mathrm{d}\alpha}{\mathrm{d}T}\beta\right) = \ln(Af(\alpha)) - \frac{E_a}{RT} \tag{4}$$

Hence, plotting the first member of eq 4 vs $1/T$ for different heating rates and for a given conversion degree makes it possible to obtain $E_a(\alpha)$, which contains useful information about the reaction mechanisms.

For DSC measurements, the conversion degree is obtained by dividing the enthalpy at one point of the process by the total enthalpy, $\alpha = H/H_0$, and the rate of reaction is given by $\mathrm{d}\alpha/\mathrm{d}t = \Phi/H_0$, where Φ is the heat flow and H_0 is the enthalpy of the whole process.

Further and precise details on the way to perform such sort of calculations can be found in refs 17, 18, and 21−24.

Results and Discussion

The thermal behavior of 125 mg mL^{-1} poly(Val-Pro-Gly-Val-Gly) and poly(Val-Pro-Ala-Val-Gly) water solutions has been studied first under a three-step cyclic DSC run with a heating, then a cooling, and finally a heating again. Typical results (heating rate 8 °C min^{-1}, cooling rate −8 °C min^{-1}) of these cyclic temperature

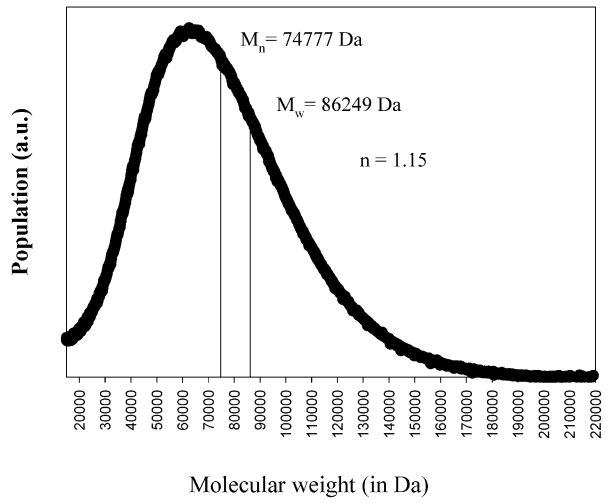

Figure 2. Apparent molecular weight distribution for poly-(Val-Pro-Ala-Val-Gly).

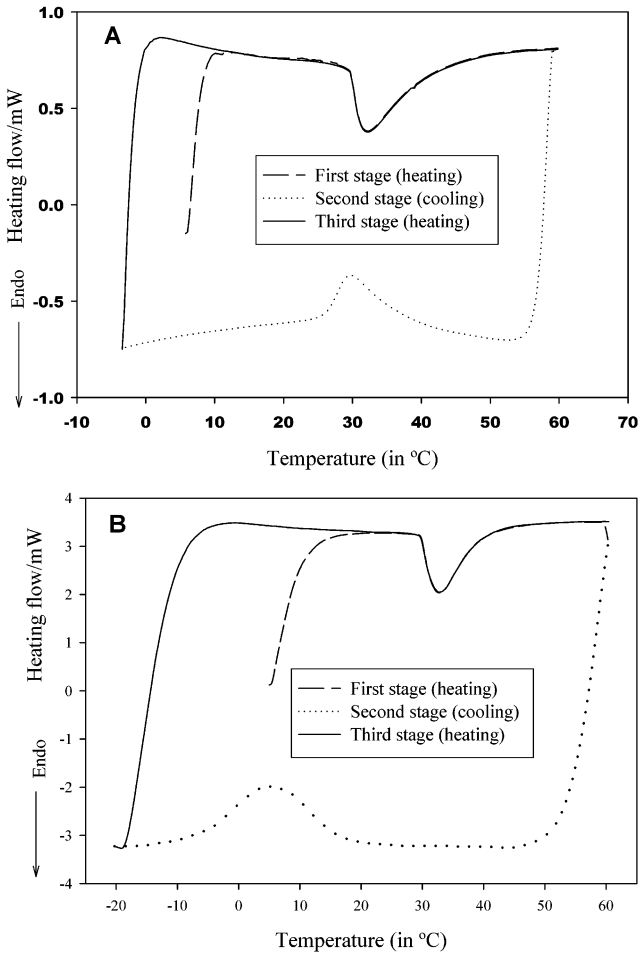

Figure 3. Typical DSC run of 125 mg mL^{-1} samples standing the heating−cooling−heating cyclic temperature program described in the text: (A) poly(Val-Pro-Gly-Val-Gly); (B) poly-(Val-Pro-Ala-Val-Gly). Heating rates of 8 and −8 °C min^{-1} cooling were used in this example.

programs have been plotted in Figure 3 for poly(Val-Pro-Gly-Val-Gly) and poly(Val-Pro-Ala-Val-Gly). The patterns shown by both polymers share common features. During the first heating run, the presence of an endothermic transition is evident for both polymers. This endotherm is caused by the characteristic process of chain folding, which is accompanied by the destruction of the ordered shell of NPS. Obviously, this last endothermic contribution dominates this calorimetric run.[13,15] T_t can be identified as the peak temperature. On the contrary, the subsequent cooling stage shows a clear exotherm for both polymers. This reflects the reverse process; i.e., the unfolding of the polymer chain and its concurrent NPS shell formation. However, although the main features are common for both polymers, there are significant differences that point to their divergent behavior. For poly(Val-Pro-Gly-Val-Gly), heating T_t ("T_{tH}") and cooling T_t ("T_{tC}") show only marginal differences that can be attributed to the inherent thermal lags of the DSC experiment (see Figure 3A). However, for poly(Val-Pro-Ala-Val-Gly), the difference $T_{tH} - T_{tC}$ scores 25.6 °C for this cycle run at 8 °C min^{-1} (T_{tH} = 30.7 °C and T_{tC} = 6.1 °C) (see Figure 3B). This indicates that a clear hysteresis behavior exists for poly(Val-Pro-Ala-Val-Gly); the polymer chain folds at 30.7 °C but does not unfold until the temperature is undercooled to 6.1 °C. Additionally, the difference $T_{tH} - T_{tC}$, i.e., the degree of undercooling, for poly(Val-Pro-Ala-Val-Gly) is found to be, to a significant extent, heating/cooling rate dependent. This is specially true for T_{tC}. This difference increases with the heating/cooling rate, being larger than 15 °C at the lower rates. To assess the actual differences and confirm the DSC results, T_{tH} and T_{tC} values were also obtained under static conditions by performing turbidity measurements. In this experimental approach, T_t is considered as the temperature yielding a 50% turbidity increase. These results are plotted in Figure 4 for poly(Val-Pro-Ala-Val-Gly). The turbidity values found for this polymer were T_{tC} = 17.5 °C and T_{tH} = 30.3 °C. Thus, even under static measurements, a difference of 12.8 °C was found, which clearly points to that the differences found by the DSC technique are to a great extent caused by the specific molecular characteristics of poly(Val-Pro-Ala-Val-Gly) and not exclusively attributable to artifacts, kinetic effects, or experimental conditions.

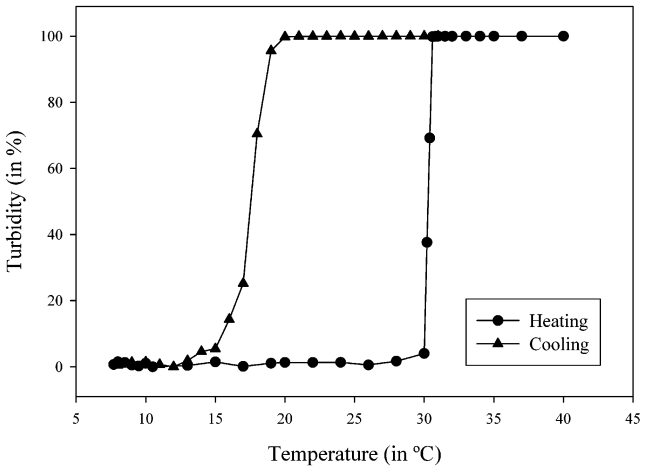

Figure 4. Turbidity profiles for a 32.1 mg mL^{-1} poly(Val-Pro-Ala-Val-Gly) water solution.

Enthalpy ("ΔH") values associated with the above calorimentric transitions also show remarkable differences between poly(Val-Pro-Gly-Val-Gly) and poly(Val-Pro-Ala-Val-Gly). ΔH values found for the different heating and cooling rate experiments are summarized in Table 1. Poly(Val-Pro-Gly-Val-Gly) shows a transition ΔH = 10 J g^{-1}; this absolute value is the same within the experimental error regardless of the heating or cooling sense or the different dynamic conditions con-

Table 1. ΔH_C and T_t for Poly(Val-Pro-Ala-Val-Gly) at Different Cooling Rates

cooling rate (°C min^{-1})	T_t (°C)	ΔH_C (J g^{-1})
−2	14.30	66.15
−4	10.80	72.52
−8	6.14	82.98
−12	2.05	85.76
−16	0.47	91.21

sidered. However, poly(Val-Pro-Ala-Val-Gly) shows clear dissimilar ΔH values for heating ("ΔH_H") and cooling ("ΔH_C"). For all cooling and heating rates used in the study, ΔH_H shows a practically constant value $\Delta H_H = 34$ J g^{-1}. On the contrary, ΔH_C is strongly cooling rate dependent, being higher at higher cooling rates (see Figure 5); ΔH_C is always ca. 2−3 times higher than ΔH_H.

Interestingly, and in an intriguing counterintuitive manner, the enthalpy excess found on cooling does not seem to reproduce during a subsequent heating run. In this way, during the third run (second heating scan) shown in Figure 3B, ΔH_H matches that of the first run at 34 J g^{-1}, while ΔH_C was of 83 J g^{-1}. In fact, the endothermic peaks found during the first and third stages are totally alike in all aspects, so they superimposed perfectly. The same qualitative result has been found for any of the heating and cooling rates used in this work (results not shown). This enthalpy excess measured on cooling could be attributed to the formation of some water NPS structures with a strong kinetic dependence. In this sense, this solvation excess shows characteristics that strongly depend on dynamic aspects and that on heating are not determined because they vanish all along the heating process with an endothermic contribution that spreads along the whole baseline and without contributing to the proper endothermic peak.

This behavior of poly(Val-Pro-Ala-Val-Gly) can be ascribed at the molecular level to the substitution of the first glycine of poly(Val-Pro-Gly-Val-Gly) by L-alanine. As mentioned above, and according to Urry's model,[13] the pair Pro-Gly in poly(Val-Pro-Gly-Val-Gly) is directly involved in the formation of β-turns. These β-turns are key points in the folding−unfolding process since chain folding occurs via formation of one of these β-turns per pentamer, while the complete unfolding involves the destruction of all β-turns in the chain. The optimal stereosequence for a type II β-turn is L−D. A gly residue, being achiral, can easily replace a D-residue. Therefore, the substitution of that Gly by L-Ala could be cause of significant differences in the folding state of both polymers. However, in a recent work,[25] the structure and dynamics of the same polymers used in this work were studied at various temperatures by using ^{1}H, ^{2}H, ^{13}C, and ^{15}N NMR spectra. Signal assignments were made using COSY, NOESY, HXCORR, HSQC, HMBC, and SSLR INEPT techniques. Temperature-induced conformation changes were studied using $^3J_{NHCH}$ couplings, NOESY connectivity, chemical shifts, and signal intensities. As a result of all these experimental approaches, the same physical states were discerned in different temperature regions for both polymers. In particular, a structure characterized by a β-turn stabilized by H-bonding between the Ala carbonyl and the first Val NH groups of poly(Val-Pro-Ala-Val-Gly) was detected by NOESY just above T_t.[25] Therefore, despite the L chirality of Ala, the methyl group is not so bulky to impede the formation of the β-turn. However,

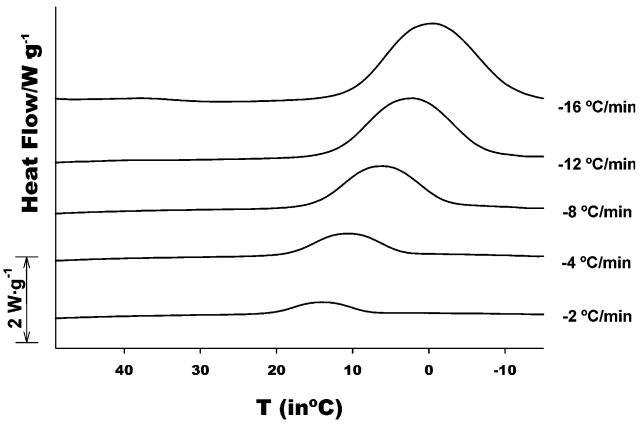

Figure 5. DSC thermograms obtained on cooling 125 mg mL^{-1} poly(Val-Pro-Ala-Val-Gly) water solutions at different cooling rates, as indicated in the plot.

according to the behavior observed in this work, it seems to hinder the process of folding and unfolding to some extent. In this sense, and according to our data, the negative influence of this methyl group seems to be more evident during the unfolding process. The presence of L-alanine seems to delay the unfolding on cooling, so chain unfolding does not occur until a strong undercooling is reached. This undercooled situation seems to promote a predominantly far-from-equilibrium situation that finally leads to the formation of a hydration excess that has not a proper thermodynamic nature.

The unexpected behavior found in the above experiments points to the necessity of elucidating the kinetic aspects of these phenomena. However, because of the assumed complex nature of the hydration−dehydration process, which proceeds in a condensed phase and with the concurrence of chain unfolding−folding and phase segregation, the use of simple models to study these kinetics seems totally inadequate. Therefore, a model-free kinetic analysis, the isoconversional Friedman method, was used to approach these phenomena. By using a model-free method, the interpretation of the results becomes not so straightforward, though the analysis will definitely result more reliable. As described in the Experimental Section, the method provides values of $E_a(\alpha)$. From the shape and values of $E_a(\alpha)$, one can speculate on a more satisfactory basis about the molecular processes involved.

The kinetic analysis, carried out as described in the Experimental Section, yielded the two $E_a(\alpha)$ functions plotted in Figure 6A for poly(Val-Pro-Gly-Val-Gly), i.e., one for the hydration−unfolding of the polymer during a cooling event ("E_{aC}") and one for the reverse dehydration−refolding process on heating ("E_{aH}"). As expected, E_{aC} showed negative values due to negative variation of the temperature during the cooling experiments; nevertheless, it is the absolute value what is of concern for the purpose of the analysis. In this case, both E_{aC} and E_{aH} showed clear variations as the conversion completes. This unambiguously indicates that, as presumed, the two processes must be considered as complex multistep processes that cannot be satisfactorily described by conventional kinetic models and analysis.

Consequently, the choice of a model-free kinetic analysis is sufficiently justified despite its more complex procedure and the lack of an absolute interpretation of the data. E_{aH}, which describes the process of chain folding and its concurrent dehydration, begins showing

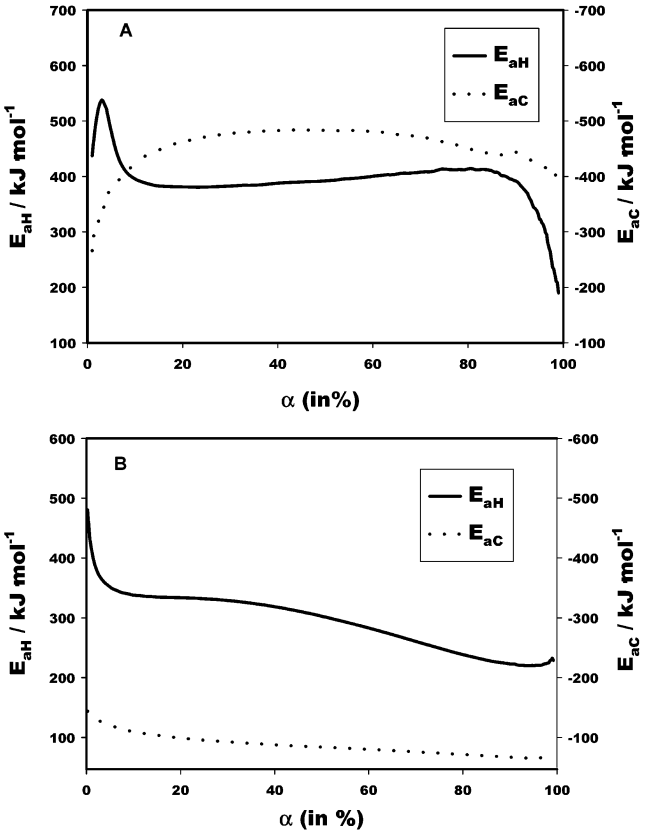

Figure 6. Activation energies as a function of α for (A) poly(Val-Pro-Gly-Val-Gly) and (B) poly(Val-Pro-Ala-Val-Gly).

high values (around 537 kJ mol^{-1}), indicating an initial slow kinetics. However, the process rapidly accelerates as it is observed a substantial decrease in E_{aH} to a level around 380 kJ mol^{-1}. This value is virtually sustained during the rest of the conversion with only a slight increase from roughly $\alpha = 20\%$ to $\alpha = 80\%$. This kind of plateau indicates the existence of a limiting step in this part of the process that conditions the overall kinetic processes within this conversion range. From this kinetic analysis, it is not possible to determine which is this limiting step. However, in many other processes involving water, the diffusion of water molecules is claimed to be the limiting step.[17,23] If this is also the case here, the diffusion of water from the surface of the destroying NPS structures to the bulk could also be the occurring limiting step. However, we have to bear in mind the complex and peculiar nature of the processes involved here. Thus, other steps, such as the chain folding itself, could as well be a plausible limiting stage. In the last part of the conversion, beyond $\alpha = 80\%$, the process further accelerates, and a final drop in E_{AH} is finally displayed (see Figure 6A). In general terms, the shape of the E_{aH} curve is of the type exhibited by most of the reversible processes.[17,23]

The trend shown by poly(Val-Pro-Gly-Val-Gly) E_{aC} shares common features with E_{aH}, but it also shows remarkable differences (see Figure 6A). Thus, and contrary to what happened in the first stages of E_{aH}, the cooling kinetics shows low E_{aC} values (260 kJ mol^{-1}). However, these low values are readily lost and an intense increase in E_{aC}, up to 480 kJ mol^{-1}, is observed during the first 20% of the conversion. Around $\alpha = 8\%$, the absolute value of E_{aC} is higher than E_{aH}, indicating that, for a great part of both processes, the unfolding and hydration of the chain show a slower kinetics that its reverse process of refolding and dehydration. Beyond $\alpha = 20\%$, the E_{aC} curve shows a plateau, although a convex-like shape is displayed over the whole curve. Again, the presence of a more or less defined plateau would seem to indicate the existence of a limiting step during most of the process. In addition, this convex shape has been identified in many different systems with a limiting diffusion step.[17,23] Thus, it is plausible to think that water diffusion from the bulk to the newly formed NPS structures is a limiting step for the process of chain unfolding and hydration of the polymer.

The situation found for poly(Val-Pro-Ala-Val-Gly) showed similarities but also significant differences to poly(Val-Pro-Gly-Val-Gly). The evolution of poly(Val-Pro-Ala-Val-Gly) E_{aH} and E_{aC} has been plotted in Figure 6B. E_{aH} shows initial values around 480 kJ mol^{-1}, which rapidly decrease to 340 kJ mol^{-1} during the first moments of the conversion. From this point ahead, the E_{aH} curve tends to reach a similar plateau as observed for poly(Val-Pro-Gly-Val-Gly). However, this horizontal trend is only established up to a conversion of roughly 30%. From this point onward, E_{aH} undergoes a mild drop and only becomes stable at a value of 220 kJ mol^{-1} during the final stages, at conversions beyond 85%. According to the literature,[23] the cited shape displayed by E_{aH} perfectly resembles the typical shape of a process with a change in the limiting step. Therefore, one can reasonably assume that this circumstance is taking place during the kinetics of chain refolding and dehydration of poly(Val-Pro-Ala-Val-Gly).

On the other hand, poly(Val-Pro-Ala-Val-Gly) E_{aC} strongly differs from that found for poly(Val-Pro-Gly-Val-Gly). E_{aC} values are clearly lower than those found for poly(Val-Pro-Gly-Val-Gly), indicating that this process of chain unfolding and hydration progresses at a higher rate for poly(Val-Pro-Ala-Val-Gly) than for poly(Val-Pro-Gly-Val-Gly). In addition, E_{aC} values displayed by poly(Val-Pro-Ala-Val-Gly) are also lower that those of E_{aH}. Contrary to what was estimated for poly(Val-Pro-Gly-Val-Gly), now the process of chain unfolding/dehydration proceeds in a more rapid manner than the folding/dehydration. Finally, and in this case, the E_{aC} curve clearly shows a plateau for the practical totality of α, suggesting a strong kinetic limiting step. To provide understanding for these differences, we have to consider that, as discussed earlier, the substitution of glycine by alanine is expected to hinder the bond rotation needed to establish or destruct the β-turns, the main feature of the folded state for both polymers.[25] As found earlier, the unfolding process seems to be particularly blocked by the bulkiness of alanine and only takes place after strong undercoolings. Consequently, one should not be surprised to find out that under these circumstances of considerable undercooling, and clearly far from a thermodynamic equilibrium, the kinetics of unfolding are faster and show evidences of a limiting step.

Acknowledgment. This work was supported by the "Junta de Castilla y León" (Projects VA30/00B and VA002/02) and by the MCYT (Projects MAT2000-1764-C02-02 and MAT2001-1853-C02-01). J. Reguera was supported by a grant from the "Junta de Castilla y León" (program FPI).

References and Notes

(1) Brooks, C. L., III; Karplus, M. *J. Mol. Biol.* **1989**, *208*, 159.

(2) Makarov, V. A.; Feig, M.; Andrews, B. K.; Pettit, B. M. *Biophys. J.* **1998**, *75*, 150.
(3) Gerstein, M.; Chotia, C. *Proc. Natl. Acad. Sci. U.S.A.* **1996**, *93*, 10167.
(4) Li, B.; Alonso, D. O. V.; Bennion, B. J.; Daggett, V. *J. Am. Chem. Soc.* **2001**, *123*, 11991.
(5) Nandi, N.; Bhattacharyya, K.; Bagchi, B. *Chem. Rev.* **2000**, *100*, 2013.
(6) Jeffrey, G. A.; Saenger, W. *Hydrogen Bonding in Biological Systems*; Springer-Verlag: Berlin, 1991; p 23.
(7) Kauzmann, W. *Adv. Protein Chem.* **1959**, 141.
(8) Edsall, J. T.; McKenzie, H. A. *Adv. Biophys.* **1983**, *16*, 53.
(9) Frank, H. S.; Evans, M. W. *J. Chem. Phys.* **1945**, *13*, 493.
(10) Tanford, C. *The Hydrophobic Effect: Formation of Micelles and Biological Membranes*; John Wiley & Sons: New York, 1973.
(11) Chothla, C. *J. Mol. Biol.* **1976**, *105*, 1.
(12) Urry, D. W.; Peng, S. Q.; Xue, J.; McPherson, D. T. *J. Am. Chem. Soc.* **1997**, *119*, 1161.
(13) Urry, D. W. *Angew. Chem., Int. Ed. Engl.* **1993**, *32*, 819.
(14) Lee, J.; Macosko, C. W.; Urry, D. W. *J. Biomater Sci., Polym. Ed.* **2001**, *12*, 229.
(15) Rodríguez-Cabello, J. C.; Alonso, M.; Pérez, T.; Herguedas, M. M. *Biopolymers* **2000**, *54*, 282.
(16) Rama Rao, G. V.; Balamuragan, S.; Meyer, D. E.; Chilkoti, A.; López, G. P. *Langmuir* **2002**, *18*, 1819.
(17) Vyazovkin, S.; Wight, C. A. *Annu. Rev. Phys. Chem.* **1997**, *48*, 125−49.
(18) Brown, M. E.; Maciejewski, M.; Vyazovkin, S.; Nomen, R.; Sempere, J.; Burnham, A.; Opfermann, J.; Strey, R.; Anderson, H. L.; Kemmler, A.; Keuleers, R.; Janssens, J.; Desseyn, H. O.; Li, C. R.; Tang, T. B.; Roduit, B.; Malek, J.; Mitsuhashi, T. *Thermochim. Acta* **2000**, *335*, 125.
(19) Urry, D. W. *J. Protein Chem.* **1988**, *7*, 1.
(20) Alonso, M.; Arranz, D.; Reboto, V.; Rodríguez-Cabello, J. C. *Macromol. Chem. Phys.* **2001**, *202*, 3027.
(21) Galwey, A. K.; Brown, M. E. *Thermal Decomposition of Ionic Solids*; Elsevier: Amsterdam, 1999.
(22) Vyazovkin, S. *Thermochim. Acta* **2003**, *397*, 269.
(23) Vyazovkin, S.; Lensnikovich, A. I. *Thermochim. Acta* **1990**, *165*, 273.
(24) Friedman, H. L. *J. Polym. Sci., Part C* **1964**, *6*, 183.
(25) Kurkova, D.; Kriz, J.; Schmidt, P.; Dybal, J.; Rodriguez-Cabello, J. C.; Alonso, M. *Biomacromolecules* **2003**, *4*, 589.

MA034572Q